

BUREAU INTERNATIONAL DES POIDS ET MESURES

On-site comparison of Quantum Hall Effect resistance standards of the NMIJ/AIST and the BIPM

◆◆ Ongoing key comparison BIPM.EM-K12 ◆◆

Report on the November 2018 on-site comparison

Final report, February 2020

Pierre Gournay*, Benjamin Rolland*,
Takehiko Oe** and Nobu-Hisa Kaneko**

* Bureau International des Poids et Mesures (BIPM)

** National Metrology Institute of Japan (NMIJ/AIST), Japan



On-site comparison of Quantum Hall Effect resistance standards of the NMIJ/AIST and the BIPM

◆◆ Ongoing key comparison BIPM.EM-K12 ◆◆

1. Introduction

The ongoing on-site comparison BIPM.EM-K12 is part of the BIPM programme implemented to verify the international coherence of primary resistance standards. It allows National Metrology Institutes (NMIs) to validate their implementations of the Quantum Hall Effect (QHE) for dc resistance traceability by comparison to the reference maintained at the BIPM.

In this comparison, the realization of the ohm from the QHE-based standard of the NMIs at 100 Ω is compared with that realized by the BIPM from its own transportable quantum Hall resistance standard. This comparison is normally completed by scaling measurements from 100 Ω to 1 Ω and 10 k Ω .

The comparison programme BIPM.EM-K12 started in 1993. A first series of five comparisons was carried out from this date until 1999. After a suspension period, the comparison was resumed in 2013. Since then four comparisons have been successfully completed whose results may be consulted on the webpage of the Key Comparison Data Base (KCDB) [1].

In November 2018 a new comparison was carried out at the National Metrology Institute of Japan, NMIJ/AIST. During this comparison, unusual noisy measurement conditions have been encountered, requiring the use of longer integration times than usual in both the NMIJ and the BIPM measuring systems. Considering the significant increase of the duration of a single measurement induced by those long integration times as well as the limited duration of the on-site comparison, the comparison programme had to be reduced. We gave priority to the 100 Ω calibration against the QHR and to the scaling from 100 Ω to 10 k Ω . Consequently, no comparison results regarding the scaling from 100 Ω to 1 Ω will be presented in this report.

2. Principle of the comparison measurements

The ohm can be reproduced from the QHE routinely with an accuracy of the order of 1 part in 10^9 or better. The present comparison is performed on-site in order to eliminate the limitation of transporting transfer resistance standards between the BIPM and the participating institute, which would otherwise result in an increase of the comparison uncertainty by at least a factor of 10.

To this end, the BIPM has developed a complete transportable system that can be operated at the participant's facilities to reproduce the ohm from a QHE reference at 100 Ω and scale this value to 1 Ω and 10 k Ω (meaning that not only the QHE systems are covered in this comparison but also the scaling devices).

For the reason given in the above introduction, only the calibration of the 100 Ω standard and scaling to 10 k Ω have been actually addressed in this comparison between the NMIJ and the BIPM. It then comprised only the two following stages, also schematized in Figure 1:

- (i) The calibration of a 100 Ω standard resistor in terms of the QHE based standard of each of the institutes (NMIJ and BIPM). The conventional value R_{K-90} is used to define the quantum Hall resistance value of both institutes. The relative difference in the calibrated values of the standard resistor of nominal value $R=100 \Omega$ is expressed as $(R_{NMIJ} - R_{BIPM})/R_{BIPM}$ where R_{BIPM} and R_{NMIJ} are the values attributed by the BIPM and the NMIJ, respectively. The relative difference is independent of the value used for the von Klitzing constant and remains valid in the revised SI.

- (ii) The scaling from $100\ \Omega$ to $10\ \text{k}\Omega$, through the measurement of the ratio $R_{10\text{k}\Omega}/R_{100\Omega}$ of the resistance of two standards of nominal value $10\ \text{k}\Omega$ and $100\ \Omega$. The relative difference in the measurement of this ratio, hereinafter referred to as $K1$, is expressed as $(K1_{\text{NMIJ}} - K1_{\text{BIPM}})/K1_{\text{BIPM}}$ where $K1_{\text{BIPM}}$ and $K1_{\text{NMIJ}}$ are the values attributed by the BIPM and the NMIJ, respectively.

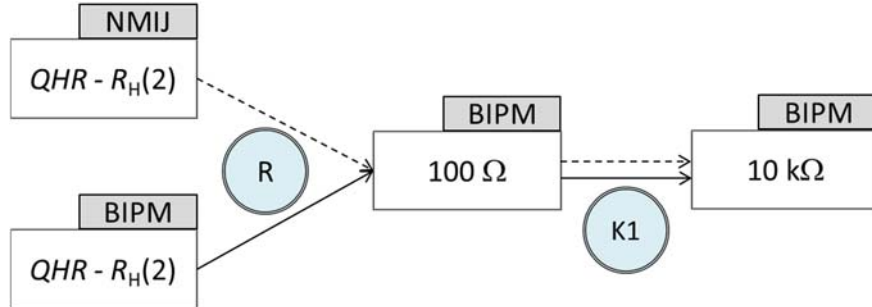


Figure 1: Schematic of the on-site comparison carried out at the NMIJ in November 2018. Rectangles represent the resistances to be compared and circles correspond to the resistance R or the ratio $K1$ to be measured. Solid and dashed arrows stand for the measurements with the 1 Hz bridge of the BIPM or with the CCC bridge of the NMIJ, respectively.

The resistance value of each of the standard resistors used in this comparison is defined as its five-terminal dc-resistance value¹. This means that it corresponds to the dc voltage to current ratio once any thermal emf across the resistor has reached a stable value.

3. The BIPM measurement system and the transfer standards

3.1. Implementation of the QHE

A complete transportable QHE reference [2] has been developed at the BIPM for the purpose of the BIPM.EM-K12 on-site comparison programme. It is composed of a compact liquid helium cryostat equipped with an 11 tesla magnet and a sample space that can be cooled to 1.3 K with the included vacuum pump. The superconducting magnet has an additional support at the bottom of the dewar to allow safe transport.

The separate sample probe can support two TO-8 mounted quantum Hall devices simultaneously (side by side within the magnet), with guarded wiring for eight terminals on each device. The BIPM uses GaAs heterostructure devices fabricated in the LEP 1990 EUROMET batch [3]. They give an $i=2$ plateau centered around 10.5 T which is well quantized for currents of at least $100\ \mu\text{A}$ at 1.5 K. The cryostat and the QHE devices are suitable for a realization of the ohm meeting all the requirements of the CCEM guidelines [4] for a relative standard uncertainty of the order of 1×10^{-9} .

A transportable resistance bridge is used with the QHE cryostat for the measurement of the different resistance ratios being the subject of the comparison. It is based on a room-temperature low-frequency current comparator (LFCC) operated at 1 Hz (sinusoidal signal), meaning that all resistance or ratio measurements are carried out at 1 Hz by the BIPM during the comparison. That way to proceed is preferable to the transport of the BIPM Cryogenic Current Comparator (CCC) bridge on-site since the 1 Hz bridge is a more rugged instrument, simple to operate, and much less sensitive to electromagnetic

¹ Ratio of the voltage drop between the high and low potential terminals to the current flowing in the low current terminal, with the case - fifth terminal - maintained at the same potential as the low potential terminal

interference and temperature variations. Furthermore, it provides resolution and reproducibility that are comparable to those achievable with the BIPM CCC bridge.

The 1 Hz bridge is equipped with two separate LFCCs of ratio 129:1 and 100:1, having turns 2065:16 and 1500:15. The construction and performance of these devices are detailed in [5,6].

3.2. Transfer standards

Two transfer resistance standards of value 100 Ω and 10 k Ω are used during the comparison. The values assigned by the BIPM and the NMIJ to the 100 Ω resistor in terms of R_{K-90} and to the ratio 10 k Ω /100 Ω are the measurands being compared in this comparison.

The transfer standards were provided by the BIPM. Both the 100 Ω and the 10 k Ω standards are Tegam resistors of type SR102 (s/n: A2030405) and SR104 (s/n: K204039730104), respectively. They are fitted in individual temperature-controlled enclosures held at 25°C. The temperature-regulation system can be powered either from the mains or from external batteries.

For each of these standards, the difference between resistance values measured at 1 Hz and at 'dc' is small but not negligible. These differences were determined at the BIPM prior to the comparison and checked after. The 'dc' value was measured with the BIPM CCC whilst the 1 Hz value with the transportable 1Hz bridge subsequently used on-site during the comparison. The differences are applied as corrections to the measurements performed at 1 Hz meaning that the 1 Hz bridge is used as a transfer instrument referenced to the BIPM CCC.

The frequency corrections (1 Hz-'dc') are reported in Table 1 for each of the two transfer standards. The main possible sources contributing to these corrections are the quantum Hall resistance (QHR), the 1 Hz bridge and the transfer standard itself. Nevertheless, at 1 Hz, the frequency dependence of the QHR is negligible compared to the comparison uncertainty [7], and the characterization of the bridge provides evidence that its error at 1 Hz is below 1 part in 10⁹. Consequently, the frequency dependence observed is mainly attributed to the resistance standards themselves.

Resistance or resistance ratio	1 Hz-'dc' correction /10 ⁻⁹	Standard uncertainty /10 ⁻⁹
$(R_{100\Omega}(1 \text{ Hz}) - R_{100\Omega}(\text{dc})) / 100$	-9.9	1.0
$(K1(1 \text{ Hz}) - K1(\text{dc})) / 100$	9.6	1.0

Table 1: Value of the 1 Hz to 'dc' corrections applied to the BIPM measurements carried out at 1 Hz. These values are specific to the standards used in the present comparison.

For the sake of completeness, it must be noticed that the 'dc' resistance value (or ratio) measured with the BIPM CCC bridge results from a current signal passing through the resistors having polarity reversals with a waiting time to zero between polarity inversions, cf. Figure 2. The polarity reversal frequency is of the order of 3 mHz (about 340 s cycle period) and the measurements are sampled only during 100 s before the change of polarity.

Previous characterization measurements of the $R_H(2)/100 \Omega$ and 10 k Ω /100 Ω ratios have shown that if the polarity reversal frequency is kept below 0.1 Hz, then any effects of settling or ac behaviour remain of the order of 1 part in 10⁹ or less.

However, in order to ensure the best possible comparability of the measurements performed by the BIPM and the participating institute, the measuring system of the latter should be configured to match as closely as possible the reference polarity reversal cycle of the BIPM CCC. In case this is not feasible, a correction should be estimated and applied if necessary to the participating institute's measurements, based on

additional characterization of the influence of the polarity reversal rate on the actual measured resistance ratio, or by any other means using the most relevant and reliable information available.

Notice that in case different reversal current cycles would have been used by the BIPM and the NMI, an estimation of the difference of the effective powers dissipated in the resistance standards measured should be done and eventually corrected taking into account the power coefficients of those standards.

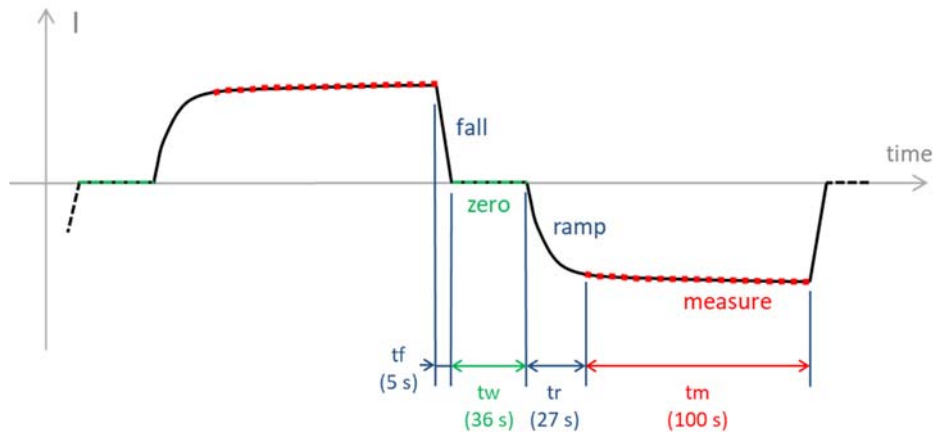


Figure 2: Schematic representation of the reference current cycle with polarity reversals used in the BIPM CCC-bridge. Each half-cycle comprises a waiting time at zero current of 36 s, a ramp time of 27 s, a measuring (sampling) time of 100 s and a fall time of 5 s. The complete reversal cycle time is 336 s.

3.3. Uncertainty budget

Table 2 summarizes the BIPM standard uncertainties for the measurement of the 'dc' value of the 100 Ω standard in terms of the recommended value of the von Klitzing constant R_{K-90} , as well as the measurement uncertainties for the 10 k Ω /100 Ω ratio ($K1$).

Information about the imperfect realization of the ratio $R_H(2)/100 \Omega$ could be found in the references [5] and [7]. Further details about the ac measurement of the QHE will be found in the review paper [9].

<i>Parameters</i>	<i>Ratio</i>	Relative standard uncertainties / 10^{-9}	
		$R_H(2)/100 \Omega$	10 k Ω /100 Ω
Reference CCC bridge			
Imperfect CCC winding ratio		1.0	1.0
Resistive divider calibration		0.5	0.5
Leakage resistances		0.2	0.2
Noise rectification in CCC		1.0	1.0
Imperfect realization of the QHR		0.8	-
Correction of the 1 Hz-to 'dc' difference		1.0	1.0
Combined type B uncertainty, u_B=		2.0	1.8

Table 2: Contributions to the combined type B standard uncertainty for the 'dc' measurement of the two mentioned resistance ratios at the BIPM.

4. The NMIJ measurement system

4.1. Implementation of the QHE

A dry dilution refrigerator equipped with a 12 T superconducting magnet was used for device cooling. The cooling power of this fridge is 250 mW at 100 mK and the usual lowest temperature of the cold finger with some TO-8 chip carriers is less than 10 mK. The insulation resistance of the wires and connectors used for the connection of the QHE device was evaluated and found to be more than $10^{13} \Omega$.

For the present comparison, the NMIJ used a GaAs/AlGaAs heterostructure device which was previously used in a commercial QHR system. The centre of the $i=2$ plateau appears around 10.5 T and the longitudinal resistance was found to be negligible for the applied currents of at least 100 μA .

4.2. Resistance bridge

A homemade Cryogenic Current Comparator (CCC) bridge was used for all the measurements performed during this comparison. The CCC was cooled down to the liquid helium temperature and its two winding ratios 2065:16 and 1600:16 were used for the measurement of $R_H(2)/100 \Omega$ and $10 \text{ k}\Omega/100 \Omega$, respectively. The bridge uses a third 1 turn winding to balance the difference of the currents flowing in the two arms of the bridge. The current through this winding was measured as the voltage drop across a 10 k Ω resistor using a multimeter. The configuration of the bridge electronics was similar to that described in [10] and a commercial dc SQUID associated with a nanovoltmeter (EM model N11) were used as current/voltage null detector.

4.3. Uncertainty budget

The NMIJ uncertainty budget is summarized in Table 3. In normal operation mode, the NMIJ CCC bridge requires measurement of the current flowing through the 100 Ω before or after the main measurement as well as the current flowing in the third 1 turn winding (voltage across 10 k Ω). The standard uncertainties for these measurements are included in Table 3.

Furthermore, the bridge electronics uses an analogue feedback system for the second and third current sources whose amplifier's gains are limited in order to prevent any oscillations and insure their stable operation. The related uncertainty is also included in the table.

<i>Parameters</i>	Relative standard uncertainties / 10^{-9}	
	$R_H(2)/100 \Omega$	10 k $\Omega/100 \Omega$
Leakage resistances of the wirings for QHR	0.7	-
CCC winding ratio	5.0	5.0
Measurement of the current flowing through the 100 Ω	2.0	2.0
Null detectors resolution	5.0	5.0
Combined type B uncertainty, u_B=	7.4	7.3

Table 3: Contributions to the combined type B standard uncertainty for the NMIJ measurement of the two mentioned resistance ratios.

5. Measurement of the 100 Ω transfer standard in terms of $R_H(2)$

5.1. BIPM measurements

5.1.1. Preliminary tests

The quantum Hall sample used during the present comparison was operated on the $i=2$ plateau at a temperature of 1.3 K and with a rms current of 40 μA . The magnetic flux density corresponding to the middle of the plateau was determined by recording the longitudinal voltage V_{xx} versus flux density and was found to be 10.3 T. The two-terminal Hall resistance of the four-terminal-pairs device was checked before and after each series of measurements, showing that the contact resistance was smaller than a few ohms (and in any case not larger than 5 Ω - measurements limited by the resolution of the DVM used).

The absence of significant longitudinal dissipation along both sides of the device was tested as described in [4] section 6.2, by combining the measurements obtained from four different configurations of the voltage contacts (two opposite pairs in the center and at the end of the sample, and two diagonal configurations). The absence of dissipation was demonstrated within 6×10^{-10} in relative terms with a standard deviation of the same order. Subsequent series of measurements were taken from the central pair of contacts only.

5.1.2. BIPM results

As mentioned above, an rms current of 40 μA was applied to the quantum Hall device. The current in the 100 Ω transfer standard was then 5.16 mA, corresponding to a Joule heating dissipation of about 2.7 mW.

After a preliminary set of test measurements on November 14, 2018, a series of three measurements of the 100 Ω standard was interleaved with three measurements by NMIJ on November 15, 2018. A longer series of five BIPM measurements interleaved with five NMIJ measurements was carried out on November 16, 2018.

The 1 Hz-measured and dc-corrected values of the 100 Ω standard are reported in Table 4. They are expressed as the relative difference from the 100 Ω nominal value: $(R_{\text{BIPM}}/100 \Omega) - 1$.

Each of the measurements reported in the table corresponds to the mean value of 12 individual measurements corresponding to a total integration time of about 40 minutes. This is about twice the typical integration time commonly used by the BIPM. As already mentioned earlier, the reason is mainly a noise level significantly higher than usually met either at the BIPM or during other on-site comparisons.

Investigations performed at the time of the comparison didn't reveal the source of this unusual noise superimposed on the bridge balance signal. A similar observation has been made on NMIJ measurements which obliged them to use even longer integration times. It was concluded that this unusual noise level was probably due to electromagnetic disturbances coming from outside but in the vicinity of the laboratory where the measurements were carried out.

Notice that in Table 4, the 'dispersion' associated with each of the measurements corresponds to the standard deviation of the mean of the 12 individual measurements. The type A uncertainty associated with the mean value of a given day of measurements was estimated as the standard deviation of all the measurements performed on that day.

Date	Time	$(R_{\text{BIPM}}/100 \Omega) - 1 / 10^{-6}$		Dispersion $/10^{-6}$
		1 Hz measurements	'dc' corrected (1 Hz-'dc' correction)	
15/11/2018	11:33	-0.623 2	-0.613 3	0.000 6
	14:57	-0.630 5	-0.620 6	0.000 6
	17:50	-0.625 2	-0.615 3	0.000 7
Mean value =			-0.616 42	
Estimated standard deviation, u_A =			0.003 8	
16/11/2018	09:50	-0.625 1	-0.615 2	0.000 4
	12:21	-0.624 4	-0.614 5	0.000 5
	14:46	-0.625 3	-0.615 4	0.000 4
	17:15	-0.627 7	-0.617 9	0.000 7
	19:47	-0.630 4	-0.620 5	0.000 7
Mean value =			-0.616 71	
Estimated standard deviation, u_A =			0.002 5	

Table 4: BIPM measurements of the 100 Ω standard in terms of $R_{\text{H}}(2)$, on November 15 and 16, 2018. Results are expressed as the relative difference from the nominal 100 Ω value. The time corresponds to the mean time of measurement.

The R_{BIPM} values reported below correspond to the mean of the resistance measurements carried out by the BIPM on November 15 and 16, 2018.

BIPM result on **November 15, 2018**: $R_{\text{BIPM}} = 100 \times (1 - 0.616 4 \times 10^{-6}) \Omega$

Relative standard uncertainty: $u_{\text{BIPM}} = 4.3 \times 10^{-9}$

where u_{BIPM} is calculated as the quadratic sum of $u_A = 3.8 \times 10^{-9}$ and, from Table 2, $u_B = 2.0 \times 10^{-9}$.

BIPM result on **November 16, 2018**: $R_{\text{BIPM}} = 100 \times (1 - 0.616 7 \times 10^{-6}) \Omega$

Relative standard uncertainty: $u_{\text{BIPM}} = 3.2 \times 10^{-9}$

where u_{BIPM} is calculated as the quadratic sum of $u_A = 2.5 \times 10^{-9}$ and, from Table 2, $u_B = 2.0 \times 10^{-9}$.

5.2. NMIJ measurements of $R_{\text{H}}(2)/100 \Omega$

5.2.1. Preliminary tests

The contact and longitudinal resistances of the QHR device were measured before the main measurement. The contact resistances were measured by using a 3-terminal method and a current of 5 μA . All the contact pads showed small contact resistance less than 0.5 Ω from 10 to 20 mK and at the centre of $i=2$ plateau. The longitudinal resistances were measured by applying a current of 20 μA at both sides of device and were found to be less than 0.5 m Ω . In addition to this, the flatness of the plateau was briefly checked by measuring the Hall and longitudinal resistance curves against the magnetic field.

5.2.2. Power coefficient of the 100 Ω resistor

For routine measurements of ratios $R_{\text{H}}(2)/100 \Omega$ and 100 $\Omega/10 \text{ k}\Omega$ at NMIJ, the current drawn by the 100 Ω standard is 2.7 mA. This value has then also been used for this comparison by NMIJ while the BIPM used an rms current value of 5.16 mA.

In order to take into account the difference of power dissipated in the 100 Ω standard, an estimation of the power coefficient was performed by the BIPM during the comparison. This estimation was simply deduced from the measurement of the $R_H(2)/100 \Omega$ ratio at two different applied currents.

The estimated value was (-0.7 ± 1.9) ppb/mW which is in good accordance with previous estimations made during previous onsite comparisons: (-0.7 ± 0.2) ppb/mW [8] and (-0.8 ± 0.3) ppb/mW [11].

Considering the present and past determinations of the power coefficient of the 100 Ω standard, we have estimated the power coefficient in this comparison to -0.7 ppb/mW with a standard uncertainty of 0.6 ppb/mW.

5.2.3. Influence of the measurement cycle shape

The typical current reversal cycle used for routine measurements at the NMIJ is shown in Figure 3. One half cycle is composed of a ramp time (t_r), a settle time during which the current is stabilizing (t_s), a measurement or sampling time (t_m) and a fall time to zero of equal duration as the ramp time. For the measurement of the ratio $R_H(2)/100 \Omega$, t_r was fixed to 20 s, t_s to 40 s and t_m to 60 s, for a total reversal cycle duration of 280 s.

The influence of the difference between the current reversal cycle shapes and durations used by the BIPM and the NMIJ has been taken into account by computing the difference of the effective powers dissipated in each of these cycles (from the electrical energies transferred to the 100 Ω standard during the effective cycle time duration).

Considering the current cycle shapes and durations shown in Figures 2 and 3, and the respective current magnitudes used by the BIPM and the NMIJ, the difference of effective powers was estimated to be 1.27 mW. Using the power coefficient estimated in the previous section, we can then estimate a power correction on NMIJ measurements equal to (0.9 ± 0.6) ppb.

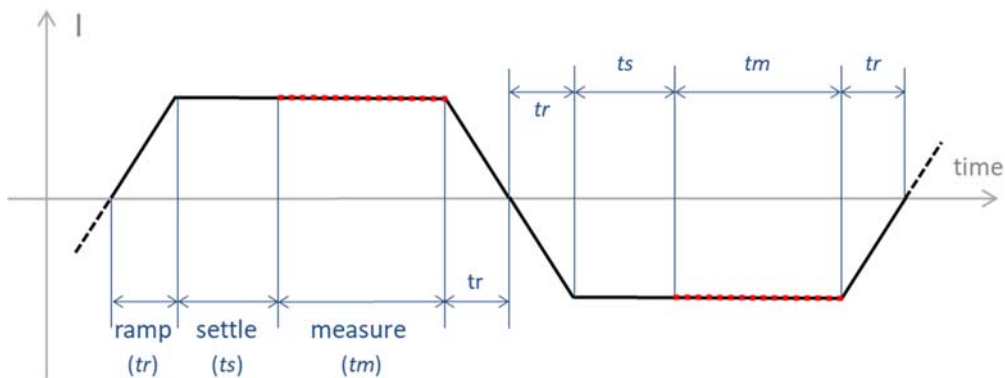


Figure 3: Typical current waveform and reversal cycle timing of the NMIJ CCC defining the ramp time (t_r), settle time (t_s) and measurement time (t_m) of the standard cycle used for measurements.

5.2.4. NMIJ results

On November 15 and 16, 2018, series of three and five measurements of the $R_H(2)/100 \Omega$ ratio were performed by NMIJ, respectively. The current in the QHR was 21 μA corresponding to 2.7 mA in the 100 Ω standard. Those measurements were interleaved with the BIPM measurements shown in Table 4. Each of the NMIJ measurements was the mean value of 28 independent measurements corresponding to a mean integration time of 56 minutes. As already discussed in section 5.1.2, such a long integration time was necessary to reach an acceptable type A uncertainty.

The measurement results of NMIJ are summarized in Table 5. The 'dispersion' associated with each of the measurements corresponds to the standard deviation of the mean of the 28 independent measurements.

The type A uncertainty associated with the mean value of a given day of measurements was estimated as the standard deviation of all the measurements performed on that day.

Date	Time	$(R_{\text{NMIJ}}/100 \Omega) - 1 / 10^{-6}$		Dispersion $/10^{-6}$
		Raw measurements	'Power' corrected	
15/11/2018	13:14	-0.616 0	-0.6151	0.004 9
	16:26	-0.619 3	-0.6184	0.004 5
	19:47	-0.612 7	-0.6118	0.005 6
Mean value =			-0.615 10	
Estimated standard deviation, u_A =			0.003 3	
16/11/2018	08:29	-0.610 8	-0.6099	0.007 7
	11:11	-0.609 3	-0.6084	0.006 9
	13:28	-0.617 1	-0.6162	0.006 7
	16:00	-0.615 5	-0.6146	0.004 8
	18:36	-0.624 2	-0.6233	0.005 0
Mean value =			-0.614 48	
Estimated standard deviation, u_A =			0.005 9	

Table 5: NMIJ measurements of the 100 Ω standard in terms of $R_{\text{H}}(2)$ on November 15 and 16, 2018. Results are expressed as the relative difference from the nominal 100 Ω value. The time corresponds to the mean time of measurement.

The R_{NMIJ} values reported below correspond to the mean of the resistance measurements carried out by the BIPM on November 15 and 16, 2018.

NMIJ result on **November 15, 2018:** $R_{\text{NMIJ}} = 100 \times (1 - 0.6151 \times 10^{-6}) \Omega$

Relative standard uncertainty: $u_{\text{NMIJ}} = 8.1 \times 10^{-9}$

where u_{NMIJ} is calculated as the quadratic sum of: $u_A = 3.3 \times 10^{-9}$, of $u_p = 0.6 \times 10^{-9}$ the uncertainty on the power correction and, from Table 3, $u_B = 7.4 \times 10^{-9}$.

NMIJ result on **November 16, 2018:** $R_{\text{NMIJ}} = 100 \times (1 - 0.6145 \times 10^{-6}) \Omega$

Relative standard uncertainty: $u_{\text{NMIJ}} = 9.5 \times 10^{-9}$

where u_{NMIJ} is calculated as the quadratic sum of: $u_A = 5.9 \times 10^{-9}$, of $u_p = 0.6 \times 10^{-9}$ the uncertainty on the power correction and, from Table 3, $u_B = 7.4 \times 10^{-9}$.

5.3. 100 Ω measurements comparison

Figures 4 and 5 present the corrected interleaved measurements from NMIJ and BIPM on November 15 and 16, 2018 (from data in Tables 4 and 5). Error bars correspond to the dispersion observed for each measurement.

On both figures it can be noticed that there is a slight non-linear drift of the measured value of the 100 Ω standard with time which could be due - but without any certainty - to the temperature variation of its resistance, not fully compensated by its temperature control electronics. However, the residual ratio variations are well followed by the BIPM and NMIJ measuring systems on the whole day of measurement. Therefore, we considered that the mean values of the series of measurements could be directly compared

and no additional uncertainty component related to these small variations was included in the final comparison results (notice that, for the BIPM, the influence of these variations is taken into account anyway as the dispersion of one single measurement is significantly smaller than the computed type A uncertainty of the series of measurements – see Table 4).

The difference between the NMIJ and the BIPM was then calculated as the mean of the differences computed from measurements obtained on November 15 and 16, 2018. The differences and their mean as well as the associated relative combined uncertainties are reported in Table 6.

As the type A uncertainty of the two relative differences $(R_{NMIJ} - R_{BIPM})/R_{BIPM}$ obtained from measurements on 15 and 16 November are uncorrelated, the combined uncertainty u_{comp} is computed as,

$$u_{comp} = \left[u_{B,NMIJ}^2 + u_{B,BIPM}^2 + \left(\frac{u_{A,15Nov}^2 + u_{A,16Nov}^2}{4} \right) \right]^{1/2}$$

where $u_{A,15Nov}$ and $u_{A,16Nov}$ are the root mean squared of the type A uncertainties of both the BIPM and NMIJ measurements carried out on 15 and 16 November, respectively.

Date	Relative difference NMIJ-BIPM $(R_{NMIJ} - R_{BIPM})/R_{BIPM}$	NMIJ		BIPM		RSS of the u_A
		u_A	$u_{B,NMIJ}$	u_A	$u_{B,BIPM}$	
15/11	1.32×10^{-9}	3.3×10^{-9}	7.4×10^{-9}	3.8×10^{-9}	2.0×10^{-9}	$u_{A,15Nov} = 5.0 \times 10^{-9}$
16/11	2.23×10^{-9}	5.9×10^{-9}		2.5×10^{-9}		$u_{A,16Nov} = 6.4 \times 10^{-9}$
Mean relative difference NMIJ-BIPM				1.8×10^{-9}		
Relative combined standard uncertainty, u_{comp}				8.7×10^{-9}		

Table 6: Mean relative difference between NMIJ and BIPM for the measurement of 100 Ω against $R_H(2)$ and its associated relative uncertainty calculated from the measurements carried out on November 15 and 16, 2018.

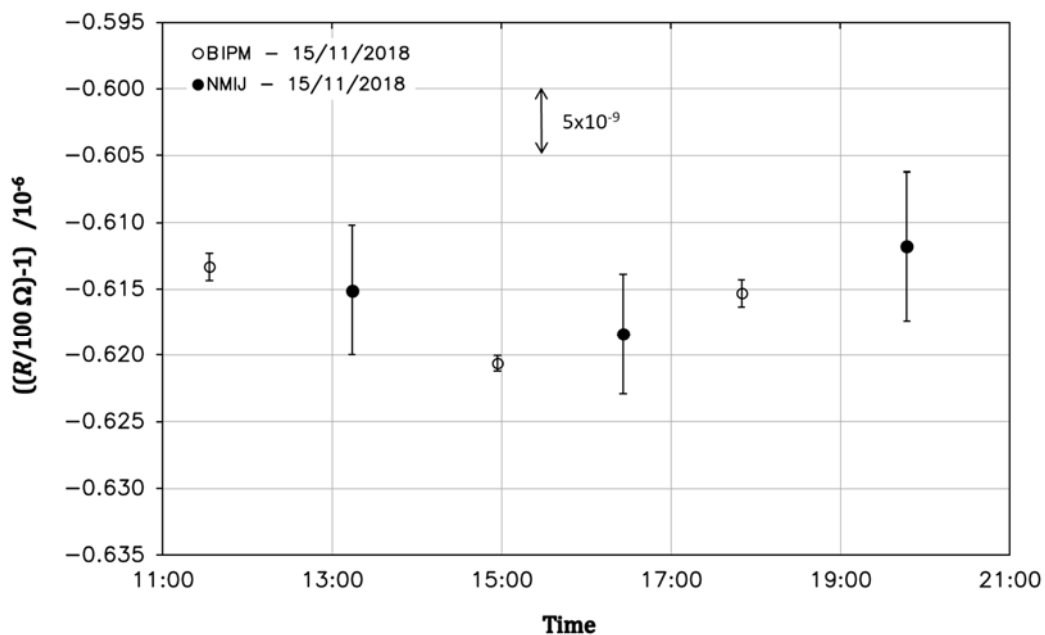


Figure 4: NMIJ (black dots) and BIPM (open circles) corrected measurements of the 100 Ω resistance R in terms of $R_H(2)$ on November 15, 2018. The uncertainty bars correspond to the dispersion observed during each measurement.

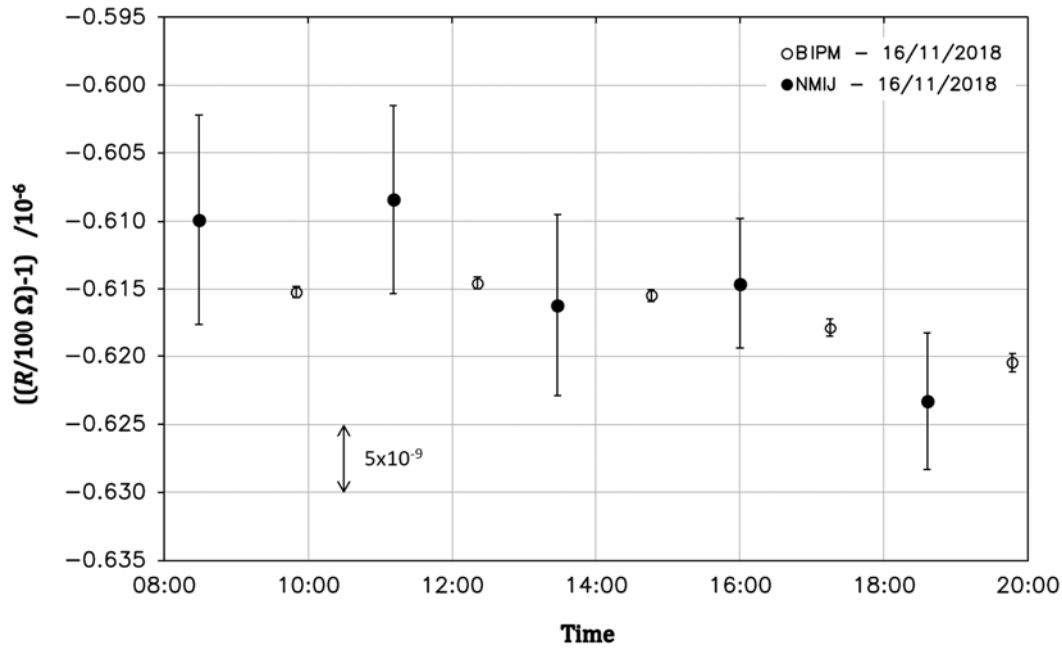


Figure 5: NMIJ (black dots) and BIPM (open circles) corrected measurements of the 100 Ω resistance R in terms of $R_H(2)$ on November 16, 2018. The uncertainty bars correspond to the dispersion observed during each measurement.

6. Measurement of the ratio $K1$ (10 kΩ/100 Ω)

6.1. BIPM measurements of $K1$

For the measurement of the $K1$ ratio the 129:1 LFCC equipping the BIPM 1 Hz bridge for $R_H(2)/100 \Omega$ ratio measurement was replaced by another one of ratio 100:1. The rms current in the 10 kΩ standard was 50 μA corresponding to 5 mA in the 100 Ω. The two standards were connected alternately to the BIPM and NMIJ bridges. Two series of interleaved measurements of $K1$ were performed on two days - November 12 and 13, 2018.

All the BIPM measurements are reported in the Table 7. Each of the measurement results corresponds to the mean value of 12 individual measurements corresponding to a total integration time of about 40 minutes. The associated dispersion corresponds to the standard deviation of the mean of the 12 individual measurements. The type A uncertainty associated with the mean value of a given day of measurements was estimated as the standard deviation of all the measurements performed on that day.

The $K1$ ratio values reported below correspond to the mean of the ratio measurements carried out by the BIPM on each of the two days, November 12 and 13, 2018.

BIPM result on **November 12, 2018**: $K1_{BIPM} = 100 \times (1 + 0.850 0 \times 10^{-6})$

Relative standard uncertainty: $u_{BIPM} = 2.2 \times 10^{-9}$

where u_{BIPM} is calculated as the quadratic sum of $u_A = 1.3 \times 10^{-9}$ and, from Table 2, $u_B = 1.8 \times 10^{-9}$.

BIPM result on **November 13, 2018**: $K1_{BIPM} = 100 \times (1 + 0.849 7 \times 10^{-6})$

Relative standard uncertainty: $u_{BIPM} = 2.1 \times 10^{-9}$

where u_{BIPM} is calculated as the quadratic sum of $u_A = 1.1 \times 10^{-9}$ and, from Table 2, $u_B = 1.8 \times 10^{-9}$.

Date	Time	$(K1_{\text{BIPM}}/100)-1 / 10^{-6}$		Dispersion $/10^{-6}$
		1 Hz measurements	'dc' corrected (1 Hz-'dc' correction)	
12/11/2018	10:03	0.857 8	0.848 2	0.000 4
	13:39	0.860 6	0.851 0	0.000 6
	17:31	0.860 1	0.850 5	0.000 4
	20:30	0.860 1	0.850 5	0.000 4
Mean value =			0.850 05	
Standard deviation, u_A =			0.001 3	
13/11/2018	09:57	0.857 7	0.848 1	0.000 4
	12:49	0.859 4	0.849 8	0.000 6
	16:57	0.860 1	0.850 5	0.000 4
	19:51	0.859 9	0.850 3	0.000 7
Mean value =			0.849 66	
Standard deviation, u_A =			0.001 1	

Table 7: BIPM measurements of the ratio $K1$ (10 000 Ω /100 Ω) on November 12 and 13, 2018. Results are expressed as the relative difference from the nominal ratio value 100. The time corresponds to the mean time of measurement.

6.2. NMIJ measurements of $K1$ ratio

6.2.1. Power correction of $K1$ ratio

NMIJ measured the $K1$ ratio with currents of 2.7 mA and 27 μA in the 100 Ω and 10 k Ω standards, respectively. These values differ from that used by the BIPM which were, as mentioned in the previous section, 5 mA and 50 μA .

The same reversal cycle as for $R_H(2)/100 \Omega$ ratio measurement (see Figure 3), but with a different ramp time, has been used by the NMIJ for the measurement of $K1$. For this measurement, t_r was fixed to 25 s, t_s to 40 s and t_m to 60 s, for a total reversal cycle duration of 300 s.

As reported in section 5.2.3, the differences of timing and magnitude of the current cycles used by the NMIJ and the BIPM were here again taken into account to estimate the difference of the effective powers dissipated in the 100 Ω standard during NMIJ and BIPM measurements. The latter was then used to compute the power correction value of $K1$ using the power coefficient of the 100 Ω discussed in a previous section (-0.7 ppb/mW). No or negligible difference of the power dissipated in the 10 k Ω standard ($\approx 18 \mu\text{W}$) is expected on the $K1$ value.

The power correction of $K1$ measurements was expected to be very close to that estimated in section 5.2.3 as both the current magnitudes and the cycle timing used by the NMIJ and the BIPM remained about the same as for the measurement of the $R_H(2)/100 \Omega$ ratio. The value was estimated to be (0.9 ± 0.6) ppb.

6.2.2. NMIJ results

On November 12 and 13, NMIJ carried out four and five measurements of the $K1$ ratio, respectively. Those measurements were interleaved with the BIPM measurements shown in Table 7. Each of the reported NMIJ values is the mean value of 28 independent measurements corresponding to a mean integration time

of 56 minutes. The reason for this long measurement time has been discussed in section 5.1.2 and was necessary to reach an acceptable type A uncertainty.

The measurement results of NMIJ are summarized in Table 8. The associated ‘dispersion’ corresponds to the standard deviation of the mean of the 28 individual measurements. The type A uncertainty associated with the mean value of a given day of measurements was estimated as the standard deviation of all the measurements performed on that day.

Date	Time	$(K1_{\text{NMIJ}}/100)-1 / 10^{-6}$		Dispersion / 10^{-6}
		Raw measurements	‘Power’ corrected	
12/11/2018	07:51	0.851 3	0.852 2	0.011 2
	11:10	0.854 5	0.855 4	0.006 4
	15:29	0.863 7	0.864 6	0.009 4
	19:12	0.858 5	0.859 4	0.009 7
Mean value =			0.857 90	
Standard deviation, u_A =			0.005 4	
13/11/2018	08:10	0.858 9	0.859 8	0.009 8
	11:34	0.853 6	0.854 5	0.012 9
	15:21	0.855 7	0.856 6	0.010 1
	18:20	0.856 5	0.857 4	0.006 6
	21:26	0.848 2	0.849 1	0.005 2
Mean value =			0.855 48	
Standard deviation, u_A =			0.004 0	

Table 8: NMIJ measurements of the (10 k Ω /100 Ω) ratio $K1$ on November 12 and 13, 2018. Results are expressed as the relative difference from the nominal ratio value 100. The time corresponds to the mean time of measurement.

The $K1$ ratio values reported below correspond to the mean of the ratio measurements carried out by the NMIJ on November 12 and 13, 2018.

NMIJ result on **November 12, 2018:** $K1_{\text{NMIJ}} = 100 \times (1 + 0.8579 \times 10^{-6})$

Relative standard uncertainty: $u_{\text{NMIJ}} = 9.1 \times 10^{-9}$

where u_{NMIJ} is calculated as the quadratic sum of $u_A = 5.4 \times 10^{-9}$, of $u_p = 0.6 \times 10^{-9}$ the uncertainty on the power correction and, from Table 3, $u_B = 7.3 \times 10^{-9}$.

NMIJ result on **November 13, 2018:** $K1_{\text{NMIJ}} = 100 \times (1 + 0.8555 \times 10^{-6})$

Relative standard uncertainty: $u_{\text{NMIJ}} = 8.3 \times 10^{-9}$

where u_{NMIJ} is calculated as the quadratic sum of $u_A = 4.0 \times 10^{-9}$, of $u_p = 0.6 \times 10^{-9}$ the uncertainty on the power correction and, from Table 3, $u_B = 7.3 \times 10^{-9}$.

6.3. Comparison of $K1$ measurements

Figures 6 and 7 present the corrected measurements from NMIJ and BIPM on November 12 and 13, 2018, respectively (data from Tables 7 and 8). Error bars correspond to the dispersion observed for each of the individual measurement.

As can be seen on those figures, no significant instability of the standards is evident and therefore no additional uncertainty component was included in the final results. The difference between NMIJ and BIPM can then be calculated as the mean of the differences computed from measurements obtained on November 12 and 13, 2018. These differences and their mean as well as the associated relative uncertainties are reported in Table 9. As the type A uncertainty of the two relative differences $(K1_{NMIJ} - K1_{BIPM})/K1_{BIPM}$ obtained from measurements carried out on 12 and 13 November are uncorrelated, the combined uncertainty u_{comp} is computed as,

$$u_{comp} = \left[u_{B,NMIJ}^2 + u_{B,BIPM}^2 + \left(\frac{u_{A,12Nov}^2 + u_{A,13Nov}^2}{4} \right) \right]^{1/2}$$

where $u_{A,12Nov}$ and $u_{A,13Nov}$ are the root mean squared of the type A uncertainties of the BIPM and NMIJ measurements carried out on 12 and 13 November, respectively.

Date	Relative difference NMIJ-BIPM $(K1_{NMIJ} - K1_{BIPM})/K1_{BIPM}$	NMIJ		BIPM		RSS of the u_A
		u_A	$u_{B,NMIJ}$	u_A	$u_{B,BIPM}$	
12/11	7.85×10^{-9}	5.4×10^{-9}	7.3×10^{-9}	1.3×10^{-9}	1.8×10^{-9}	$u_{A,12Nov} = 5.6 \times 10^{-9}$
13/11	5.82×10^{-9}	4.0×10^{-9}		1.1×10^{-9}		$u_{A,13Nov} = 4.1 \times 10^{-9}$
Mean relative difference NMIJ-BIPM					6.8×10^{-9}	
Relative combined standard uncertainty, u_{comp}					8.3×10^{-9}	

Table 9: Mean relative difference of $K1$ ratio measurements between NMIJ and BIPM and its associated relative uncertainty calculated from the measurements carried out on November 12 and 13, 2018.

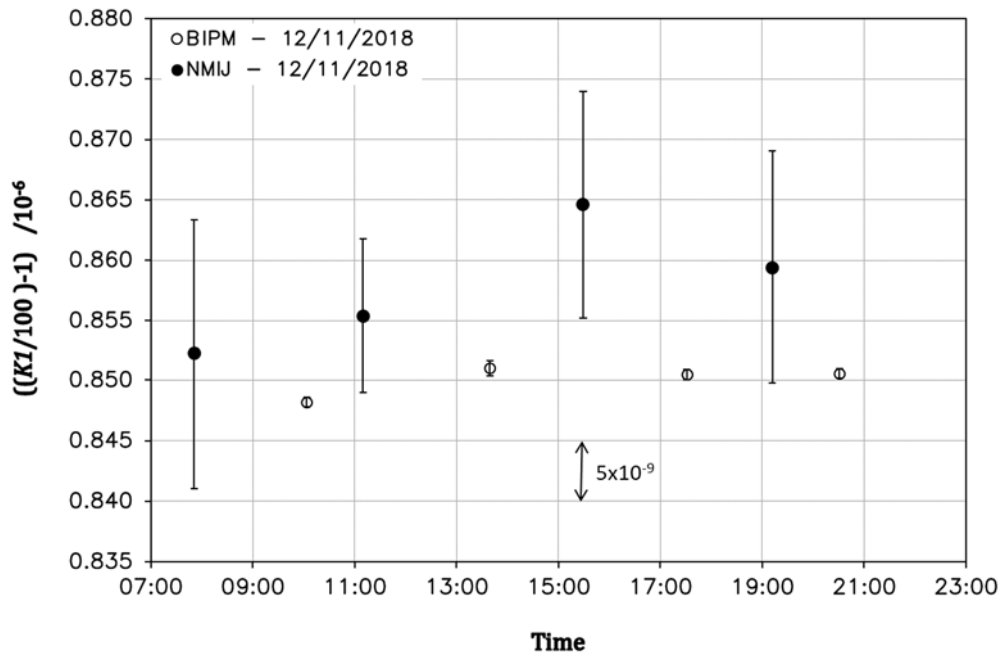


Figure 6: NMIJ (black dots) and BIPM (open circles) corrected measurements of the ratio $K1$ ($10 \text{ k}\Omega/100 \Omega$) on November 12, 2018. The error bars correspond to the dispersion observed during each measurement

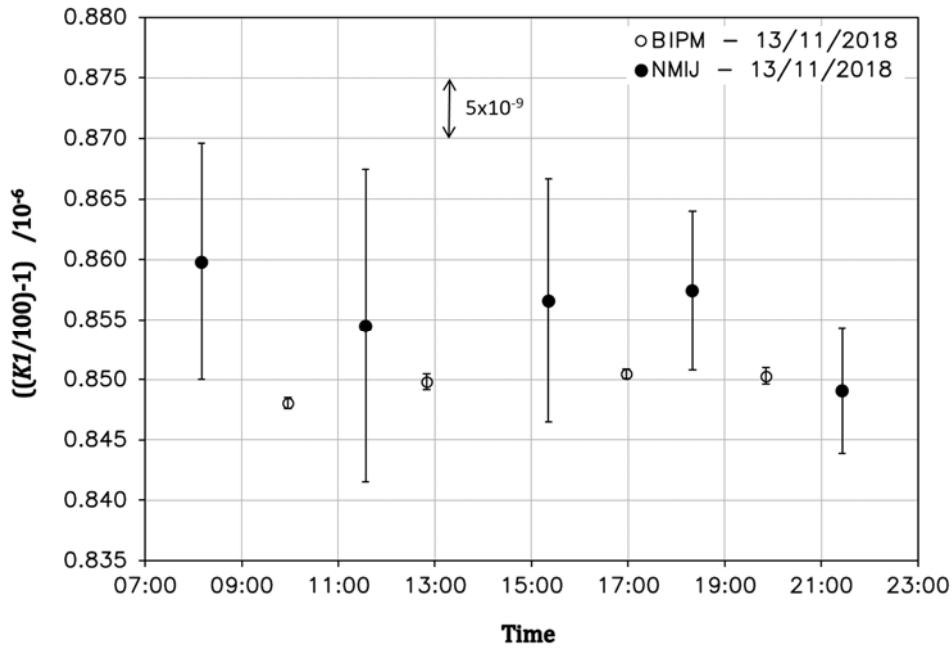


Figure 7: NMIJ (black dots) and BIPM (open circles) corrected measurements of the ratio $K1$ ($10 \text{ k}\Omega/100 \Omega$) on November 13, 2018. The error bars correspond to the dispersion observed during each measurement.

7. Conclusion

The on-site key comparison BIPM.EM-K12 carried out from November 12 to November 19, 2018 between the BIPM and the NMIJ showed a very good agreement in the measurements of a conventional 100Ω resistor in terms of the quantized Hall resistance ($R_H(2)$). A larger difference was observed in the measurement of the resistance ratio $K1$ ($10 \text{ k}\Omega/100 \Omega$) which however was still within the standard uncertainty. Nevertheless, in both cases, these results are tarnished by an unusual large comparison uncertainty - for this type of comparison - due to the large type A uncertainty components associated with the NMIJ measurements.

The results of the comparison are summarized in Table 10. The relative differences between the BIPM and the NMIJ are less than 2 and 7 parts in 10^9 for $R_{100\Omega}$ and $K1$ ratio, respectively. Relative standard uncertainties are within 8 and 9 parts in 10^9 .

$R_{100\Omega}$ in terms of $R_H(2)$	$(R_{\text{NMIJ}} - R_{\text{BIPM}}) / R_{\text{BIPM}} = \mathbf{1.8 \times 10^{-9}}$	$u_{\text{comp}} = \mathbf{8.7 \times 10^{-9}}$
$K1 = R_{10\text{k}\Omega}/R_{100\Omega}$	$(K1_{\text{NMIJ}} - K1_{\text{BIPM}}) / K1_{\text{BIPM}} = \mathbf{6.8 \times 10^{-9}}$	$u_{\text{comp}} = \mathbf{8.3 \times 10^{-9}}$

Table 10: Summary of the results and associated relative standard uncertainties of the NMIJ-BIPM onsite comparison BIPM.EM-K12.

The above results will also appear as Degree of Equivalence (DoE) in the BIPM Key Comparison Database (KCDB). The DoE of the participating institute with respect to the reference value is given by a pair of terms: the difference D from the reference value and its expanded uncertainty for $k=2$, i.e. $U=2u$. The reference value of the on-going comparison BIPM.EM-K12 was chosen to be the BIPM value.

The comparison results expressed as DoEs are summarized in Table 11.

	Difference from the reference value $D / 10^{-9}$	Expanded uncertainty $U / 10^{-9}$
$R_{100\Omega}$ in terms of $R_H(2)$	1.8	17.4
$K1 = R_{10k\Omega}/R_{100\Omega}$	6.8	16.6

Table 11: Summary of the comparison results expressed as degrees of equivalence (DoEs): difference from the BIPM reference value and expanded uncertainty U ($k=2$).

References

- [1] <https://www.bipm.org/kcdb/comparison?id=430>.
- [2] F. Delahaye, T.J. Witt, F. Piquemal and G. Genevès, "Comparison of quantum Hall effect resistance standards of the BNM/LCIE and the BIPM", *IEEE Trans on Instr. and Meas.*, Vol. 44, n°2, 1995, 258-261.
- [3] F. Piquemal, G. Genevès, F. Delahaye, J.P. André, J.N. Patillon and P. Frijlink, "Report on a joint BIPM-EUROMET project for the fabrication of QHE samples by the LEP", *IEEE Trans on Instr. and Meas.*, Vol. 42, n°2, 1993, 264-268.
- [4] F. Delahaye and B. Jeckelmann, "Revised technical guidelines for reliable dc measurements of the quantized Hall resistance", *Metrologia*, 40, 2003, 217-223.
- [5] F. Delahaye and D. Bournaud, "Accurate ac measurements of standard resistors between 1 and 20 Hz", *IEEE Trans on Instr. and Meas.*, Vol. 42, n°2, 1993, 287-291.
- [6] A. Satrapinski, M. Götz, E. Pesel, N. Fletcher, P. Gournay, B. Rolland, "New Generation of Low-Frequency Current Comparators Operated at Room Temperature", *IEEE Trans. on Instr. and Meas.*, Vol. 66, n°6, 2017, 1417-1424.
- [7] F. Delahaye, "An ac-bridge for low frequency measurements of the quantized Hall resistance", *IEEE Trans. on Instr. and Meas.*, Vol. 40, n°6, 1991, 883-888.
- [8] P. Gournay, B. Rolland, J. Kučera and L. Vojáčková, "On-site comparison of Quantum Hall Effect resistance standards of the CMI and the BIPM: ongoing key comparison BIPM.EM-K12", *Metrologia*, Vol. 54, Technical Supplement, 2017.
- [9] F. Ahlers, B. Jeanneret, F. Overney, J. Schurr and B. Wood, "Compendium for precise ac measurements of the quantum Hall resistance", *Metrologia*, 46/5, R1-R11, 2009.
- [10] J. Kinoshita, K. Inagaki, C. Yamanouchi, K. Yoshihiro, S. Kawaji, N. Nagashima, N. Kikuchi, and J.-I. Wakabayashi, "Self-Balancing Resistance Ratio Bridge Using a Cryogenic Current Comparator", *IEEE Trans. on Instr. and Meas.*, Vol. 38, n°2, 1989, 290-292.
- [11] P. Gournay, B. Rolland and C. Sanchez, "On-site comparison of Quantum Hall Effect resistance standards of the NRC-CNRC and the BIPM: ongoing key comparison BIPM.EM-K12", *Metrologia*, Vol. 56, Number 1A, Technical Supplement, 2019.